

High Magnetic Field ESR in the Haldane Spin Chains NENP and NINO

M.Sieling⁽¹⁾, U.Löw⁽²⁾, B.Wolf⁽¹⁾, S.Schmidt⁽¹⁾, S. Zvyagin⁽¹⁾ and B.Lüthi⁽¹⁾

⁽¹⁾Physikalisches Institut, Universität Frankfurt, D-60054 Frankfurt, Germany

⁽²⁾Universität Dortmund, D-44221 Dortmund, Germany

(September 28, 2018)

We present electron spin resonance experiments in the one-dimensional antiferromagnetic $S = 1$ spin chains NENP and NINO in pulsed magnetic fields up to 50 T. The measured field dependence of the quantum energy gap for $B||b$ is analyzed using the exact diagonalization method and the density matrix renormalization group method (DMRG). A staggered anisotropy term $(-1)^i d(S_i^x S_i^z + S_i^z S_i^x)$ was considered for the first time in addition to a staggered field term $(-1)^i S_i^x B_{\text{st}}$. We show that the spin dynamics in high magnetic fields strongly depends on the orthorhombic anisotropy E .

76.50.+g, 75.10.Jm, 75.40.Mg, 75.50.Ee

According to the Haldane conjecture [1] the ground-state properties and the excitation spectrum of a one-dimensional Heisenberg antiferromagnet are determined by the spin value S in a fundamental way. For integer spins the system exhibits a disordered nonmagnetic groundstate which is separated from the first excited triplet states by an energy gap, whereas half-integer spin systems have no gap. The existence of the Haldane gap has been experimentally confirmed by inelastic neutron scattering (INS) experiments [2] and magnetization measurements [3].

Electron spin resonance (ESR) experiments have proven to be an excellent method to study the magnetic field dependence of the excitation spectrum in Haldane systems [4] – [10]. In the prototypical one-dimensional spin chains $\text{Ni}(\text{C}_2\text{H}_8\text{N}_2)_2\text{NO}_2(\text{ClO}_4)$ (NENP) and $\text{Ni}(\text{C}_3\text{H}_{10}\text{N}_2)_2\text{NO}_2(\text{ClO}_4)$ (NINO) transitions between excited states have been observed at the Brillouinzone boundary at $q = \pi/b$ [4,5]. In addition transitions from the singlet groundstate at $q = 0$ to the excited triplet at $q = \pi/b$ have been found [6]–[10], which are normally forbidden by selection rules. These ESR experiments could be explained using the concept of a transverse staggered magnetic field [11,12] which mixes the eigenstates at $q = 0$ and $q = \pi/b$. Such a staggered field could be induced by an external magnetic field due to the alternating tilting of the local anisotropy axes of the Ni^{2+} ions and was first observed in NMR experiments [13]. ESR experiments are so far the only method for a direct observation of the energy gap in Haldane systems well above the critical field B_c (8.5 T in NENP and ≈ 8 T in NINO).

NENP and NINO both crystallize in the orthorhombic system and show similar lattice constants [14] – [16]. NENP can be described in the $Pnma$ space group [15] whereas NINO belongs to the $Pbn2_1$ space group [14,16]. The Ni^{2+} ions are covalently linked via NO_2 -complexes which are responsible for the antiferromagnetic superexchange interaction. Both compounds are good realizations of one-dimensional chains since the interchain exchange J' is about a factor of 10^4 smaller than the in-

trachain exchange J [14] due to the separation by the ClO_4 ions. The local surrounding of the Ni^{2+} ions is a distorted octahedron with a basal plane built out of four nitrogen atoms from the diamine groups. The axial positions are occupied by an oxygen and a nitrogen atom from the nitrite bridges. This local surrounding gives rise to a planar anisotropy D and to an orthorhombic anisotropy E as well as to an anisotropic g tensor.

A significant characteristic in NENP and NINO is the alternating tilting of the local surrounding of the Ni^{2+} ions along the chain. As we will show in this paper, it is important to know the direction of this tilting with respect to the easy direction of the orthorhombic anisotropy E . For NENP it is clear from the structure [15] and NMR experiments [13] that the tilting of the local environment is along the c direction [17] while the easy direction of the orthorhombic anisotropy is along a (see e.g. [3]). In NINO the easy direction in the basal octahedron plane is along c [18] while the structure [16] gives rise to the assumption that the local environment is tilted towards the a -axis. However it is not clear how to deduce a definite angle of tilting of the g or the D tensors out of the structure.

The ESR experiments were performed in the high magnetic field laboratory at the University of Frankfurt. Different single crystals of NENP and NINO have been mounted in a transmission type sample holder in Voigt geometry (propagation vector \vec{k} perpendicular to the external magnetic field \vec{B}) with the chain direction b parallel to \vec{B} . We used Gunn and IMPATT diodes together with frequency multipliers to produce mm-wave radiation in the frequency range 55–200 GHz. The radiation was unpolarized when passing the sample and was detected with a fast InSb hot electron bolometer mounted in a separated cryostat. High magnetic fields were produced using an Al_2O_3 strengthened copper coil with internal reinforcement, manufactured in the National High Magnetic Field Laboratory in Tallahassee, Florida. Fields up to 50 T with 8 ms rise time could be produced by discharging capacitors with a stored energy of 0.4 MJ.

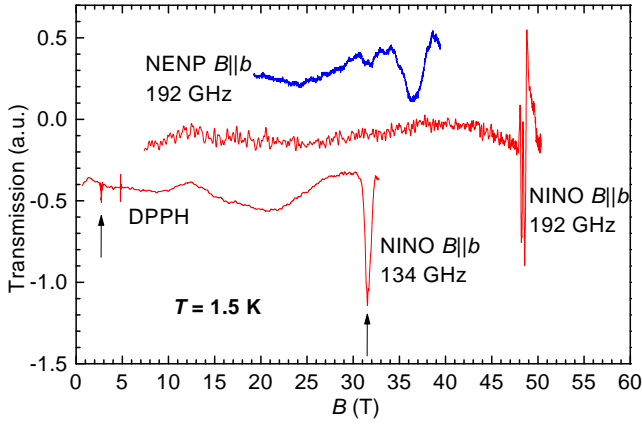


FIG. 1. Transmission spectra in NENP and NINO at $T = 1.5$ K. The arrows mark excitations from the groundstate below and above the critical field in the 134 GHz spectrum.

While the coil is operating at 77 K, the sample was cooled down to 1.5 K in a pumped ^4He cryostat. The magnetic field was measured with a pick up coil and calibrated using a DPPH reference sample. Details of the high field setup can be found in [19]

Figure 1 shows some typical mm-wave transmission spectra at $T=1.5$ K for NENP and NINO in high magnetic fields. A drastic increase of the resonance intensity can be observed with increasing field above the critical field $B_c \approx 8$ T (see corresponding arrows in fig. 1). This increase of intensity was explained before in the framework of the staggered field concept [11,12]. Also the linewidth increases remarkably in both substances: while the typical linewidth for $B < B_c$ in NENP and NINO is about 0.1 T and 0.05 T respectively, it increases for $B > B_c$ about a factor of 20 in NENP and a factor of 10 in NINO. No decrease of the integrated intensity could be observed with decreasing temperatures, indicating that the observed transitions are excitations from the groundstate [9]. The resonance frequencies therefore give a direct measure of the magnetic field dependence of the energy gap [11,12].

The frequency field dependence for all observed resonances is shown in fig. 2 together with low field data obtained by other groups. For $B < B_c$ the gap in both systems decreases with a slope corresponding to the g factor ($g_b = 2.15$ in NENP, $g_b = 2.17$ in NINO). The gap does not close but remains finite at the critical field B_c and increases again for $B > B_c$. For $B > B_c$ the curvature of the $\Delta(B)$ curve is much stronger in NENP than in NINO. The smaller slope in the high field region for NENP seems to be one explanation for the larger linewidth in this compound.

The difference in the high field spin dynamics between NENP and NINO was thought to be mainly caused by a larger staggered inclination of the Ni^{2+} surrounding in NENP [9,10] (although these assumptions are based on calculations with an isotropic Hamiltonian and unrealistically small exchange constants J). Thus the ratio of

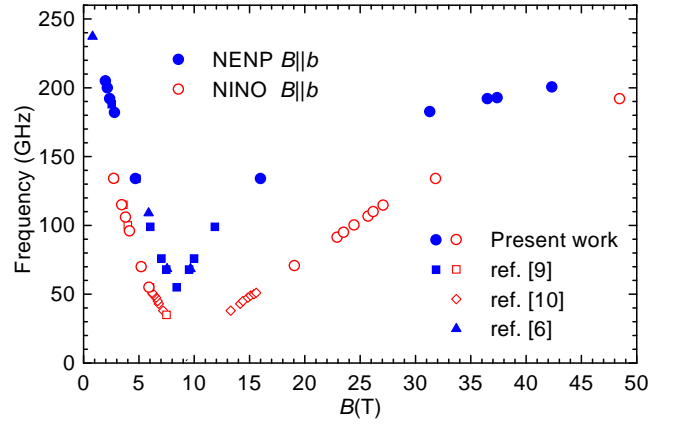


FIG. 2. Frequency field dependence of the groundstate excitations in NENP and NINO (full and open symbols respectively).

the gap energies and the ratio of the slope of the $\Delta(B)$ curves are expected to be approximately constant between B_c and $B = 4J$ [11]. In contrast the actual field dependence of the gap energies shows a different behaviour with a crossing point of both $\Delta(B)$ curves at $B = 1.8J$ (fig 3).

To analyze our data for the $B||b$ configuration more realistically we use the following Hamiltonian

$$H = \sum_i \{ J \vec{S}_i \vec{S}_{i+1} + D(S_i^z)^2 + E[(S_i^x)^2 - (S_i^y)^2] - g_z \mu_B S_i^z B + (-1)^i [d(S_i^x S_i^z + S_i^z S_i^x) + c g_z \mu_B S_i^x B] \}. \quad (1)$$

The indices x , y and z correspond to the crystallographic axes c , a and b respectively. J is the antiferromagnetic intrachain exchange, D and E are the planar and the orthorhombic anisotropies. The fourth and the following terms contain the Zeeman coupling and the *staggered* terms due to an alternating tilting of the anisotropy- and the g -tensor within the x - z plane. c is the staggered field constant $c = B_{st}/B$ which is given by the tilting angle θ_g and the difference of $g_x - g_z$:

$$c = \frac{g_x - g_z}{g_z} \frac{1}{2} \tan 2\theta_g. \quad (2)$$

d is the staggered anisotropy constant which is given by θ_D and the difference of $D - E$:

$$d = (D - E) \frac{1}{2} \tan 2\theta_D. \quad (3)$$

The parameters D , E , g_x and g_z are the observable values in the crystallographic system. They can be derived by averaging over the tilted anisotropy- and g -tensors of neighboring Ni^{2+} sites. For a more detailed derivation of (2) and (3) we refer to ref. [20].

We like to point out that although the Hamiltonian (1) contains numerous parameters, only the angles θ_g and θ_D can be considered as "free" parameters within the fitting process for our high field data. J , D and E are fixed by

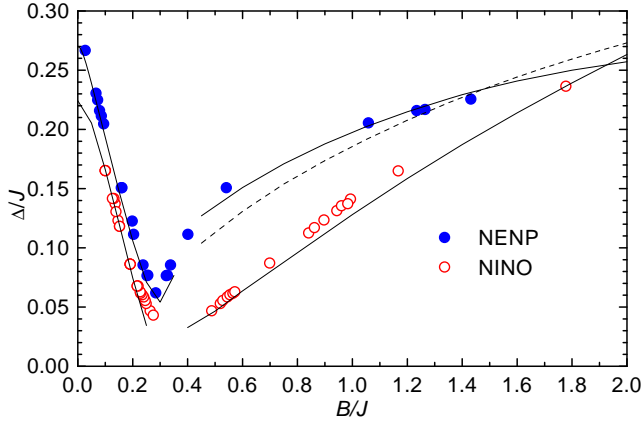


FIG. 3. Magnetic field dependence of the gap in NENP and NINO in units of J . Symbols are experimental data, lines are extrapolated numerical results based on the Lanczos method (for $B/J < 0.4$) and the DMRG method (for $B/J > 0.4$). The staggered field and anisotropy parameters are $c=-0.026$, $d/J=0.06$ and $c=0.0105$, $d/J=0.06$ for NENP and NINO respectively (solid lines). The dashed line is the best fit for NENP with $d/J = 0$ using $c = 0.017$.

the zero field size of the gaps Δ_1 , Δ_2 and Δ_3 between the groundstate and the excited triplet states at $q = \pi/b$. J is given by the well known ratio $0.41J = E_G = (\Delta_1 + \Delta_2 + \Delta_3)/3$ [21] while D and E can be deduced from the splitting of the triplet $\Delta_3 - (\Delta_1 + \Delta_2)/2$ [22] and $\Delta_2 - \Delta_1$ respectively. The gap values are taken from ESR experiments [9] which are in good agreement with INS results [2]. The g -factors for the different directions are taken from zero field susceptibility data ([15] for NENP and [18] for NINO).

Accordingly we obtain the following parameters $J=43$ K, $D/J=0.17$, $E/J=0.01$, $g_x=2.21$, and $g_z=2.15$ for NENP and $J=39$ K, $D/J=0.2$, $E/J=-0.027$, $g_y=2.23$, and $g_z=2.17$ for NINO. As noted before, in NINO the easy direction of the orthorhombic anisotropy is along the c - (x -) axis leading to a negative sign of E . Since the alternating tilting in NINO is supposed to be in the y - z plane the S_i^x operators and g_x in the staggered term of (1) have to be replaced by S_i^y operators and g_y respectively.

The magnetic field dependence of the gap was calculated both with exact diagonalization for $N=16$ spins using the Lanczos algorithm and with the density matrix renormalization group (DMRG) method. The Lanczos results for short chains can be extrapolated in a reliable way for $B < B_c$. For $B > B_c$ however the gap shows large finite size effects which manifest themselves in oscillations. This is in particular the case for small values of the staggered fields, when both the ground state energy and the first excited state energy follow almost polygonal lines as a function of B . Therefore for $B > B_c$ we use the DMRG method which allows to treat large systems with high accuracy by keeping only the most important eigenstates of a blocked density matrix constructed according

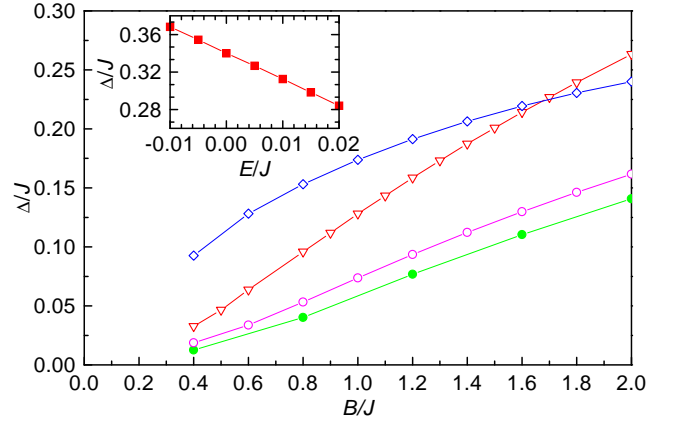


FIG. 4. Magnetic field dependence of the high field energy gap for different parameters. Full circles (●) are calculation for $c = 0.0105$, $d/J = 0$, $D/J = 0.2$ and $E/J = 0.027$. Open symbols are calculations which differ from (●) in only one parameter ((○) $c = 0.012$, (▽) $d/J = 0.06$, (◇) $E/J = 0$). The inset demonstrates the linear dependency of the gap on the orthorhombic anisotropy E at $B/J = 2$ for $c = 0.0105$, $d/J = 0.06$ and $D = 0.2$. All results are extrapolations of DMRG calculations.

to ref. [23]. We found best convergence using DMRG for $N = 40 \dots 120$ spins with open boundaries but also employed periodic boundary conditions in order to remove the $S = 1$ artefact state occurring for open boundaries in the low field range. In the high field region the method converges very well with as little as 30 states. In the region near the critical field more states and larger systems are needed.

Figure 3 shows the extrapolated results of our calculations together with the experimental data in units of J . For NINO we find $c = 0.0105$ and $d/J = 0.06$ assuming a tilting angle of $\theta_g = \theta_D = 17.5^\circ$. For NENP we obtained our best fit for $c = -0.026$ and $d/J = 0.06$ based on the tilting angles $\theta_g = -31^\circ$ and $\theta_D = 18.5^\circ$ [24] which differ in size and direction.

This somewhat strange result implies that the the g - and the D - tensors in NENP depend on different neighboring atoms of the Ni^{2+} ions, e.g. one tensor is mainly determined by the position of the nitrogen atoms of the ethylenediamine groups whereas the other tensor is principally given by the position of the nitrite bridges. A more detailed analysis is needed at this point to clarify the dependence of the g - and D -tensors on the Ni^{2+} environment. Nevertheless neglecting the staggered d term leads to a rather poor fit for the new high field data of NENP (dashed line in fig. 3) showing that this d term is essential to describe the gap as a function of the field. Besides one has to keep in mind that the interchain exchange J' was not taken into account in our calculations which possibly could affect the high field spin dynamics.

It is of special interest to study the effect of the different terms in (1) on the energy gap when varying several parameters. In a first step we checked that finite values

of c and d have practically no effect for $B < B_c$, thus confirming the values taken for J , D , and E . Next we studied the effect of c and d in the high field range. For $B > B_c$ the system is expected to be gapless without any staggered term in (1). The staggered terms lift the degeneracy between the magnetic groundstate and the first excited state in the high field phase yielding a gap which increases with B . Fig. 4 shows the gap for different c and d values as a function of field. The effect of the d term on the gap is quite small at the critical field $B_c \approx 0.4J$ but increases with B comparable with the increase of the magnetization $\sum < S_z >$ reflecting the effect of the S_i^z operators in (1).

As is well known the anisotropies D and E reduce the gap for $B < B_c$ [21], [22]. While the planar anisotropy D only has a very weak effect for $B > B_c$ it turned out that the orthorhombic anisotropy E considerably changes the size of the high field gap induced by the staggered c and d terms (fig. 4 with inset). The gap is linearly reduced for a positive E in (1) whereas it is linearly enlarged for $E < 0$ (see inset of fig. 4). The staggered c and d terms induce a staggered magnetization $\sum (-1)^i < S_i^x >$ along the x direction in NENP [11] (along the y direction in NINO), which is the hard axis of the orthorhombic anisotropy respectively. Thus a positive E increases the energy of the groundstate and the first excited states. This increase is somewhat stronger for the groundstate which shows a higher staggered magnetization than the first excited states yielding a reduction of the gap.

The orthorhombic anisotropy term is essential to describe the differences in the high field spin dynamics of NENP and NINO. As shown in fig. 4 the field dependence of the gap has a clear curvature for $E = 0$ while it becomes more linear with increasing E corresponding to the experimental results in both substances.

In the present work we have shown unprecedented data for the quantum energy gap in the Haldane systems NENP and NINO measured by ESR experiments in pulsed magnetic fields up to 50 T. We presented numerical calculations based on a direct diagonalization and the DMRG method considering the planar and orthorhombic anisotropies D and E as well as the staggered anisotropy and the transverse staggered field. The high field data could be fitted using realistic values for the exchange interaction and the anisotropies. In addition to a staggered field term the staggered anisotropy term is essential to describe the curvature of the gap as a function of field. Finally the orthorhombic anisotropy E turned out to have an unexpected strong effect on the energy gap for $B > B_c$.

Future experiments with high magnetic fields perpendicular to the chain axis could provide us with more information especially for the case where no staggered field is induced. In addition experimental and theoretical investigations on the field dependence of higher excited states should extend the knowledge about the high field phase

in these Haldane systems.

We like to thank T. Yosida and M. Date who kindly gave us the samples of NENP and NINO. This work was supported by the BMBF with the project 13N6581A/3 and by the DFG through the SFB 252. S.Z. appreciates the support of the Alexander von Humboldt Foundation.

-
- [1] F.D.M. Haldane, Phys.Lett.A **93**, 464 (1983); Phys.Rev.Lett. **50**, 1153 (1983).
 - [2] J.P. Renard *et al.*, Europhys.Lett. **3**, 945 (1987); L.P. Regnault and J.P. Renard, Phys.B 234–236, 541 (1997).
 - [3] K. Katsumata *et al.*, Phys.Rev.Lett. **63**, 86 (1989); Y. Ajiro *et al.*, Phys.Rev.Lett. **63**, 1424 (1989).
 - [4] M. Date and K. Kindo, Phys.Rev.Lett. **65**, 1659 (1990).
 - [5] L.C. Brunel *et al.*, Phys.Rev.Lett. **69**, 1699 (1992).
 - [6] W. Lu *et al.*, Phys.Rev.Lett. **67**, 3716 (1991).
 - [7] W. Palme *et al.*, Int.J.Mod.Phys. B **7**, 1016 (1992).
 - [8] T.M. Brill and J.P. Boucher, Phys.Scr. **T55**, 156 (1994).
 - [9] M. Sieling *et al.*, Z.Phys.B **96**, 297 (1995).
 - [10] M. Hagiwara and K. Katsumata, Phys.Rev.B **53**, 14319 (1996).
 - [11] T. Sakai and H. Shiba, J.Phys.Soc.J. **63**, 867 (1994); H. Shiba *et al.*, J.Magn.Magn.Mater. **140-144**, 1590 (1995).
 - [12] P.M. Mitra and B.I. Halperin, Phys.Rev.Lett. **72**, 912 (1994).
 - [13] M. Chiba *et al.*, Phys.Rev.B **44**, 2838 (1991).
 - [14] J.P. Renard *et al.*, J.Appl.Phys. **63**, 3538 (1988).
 - [15] A. Meyer *et al.*, Inorg.Chem. **21**, 1729 (1982).
 - [16] T. Yosida and M. Fukui, J.Phys.Soc.Jpn. **61**, 2304 (1992).
 - [17] In fact in NENP neighboring chains are rotated about the chain axis b by approximately $\pm 30^\circ$ leading to different local and crystallographic symmetry axes. Here we just discuss the $B||b$ configuration and therefore will neglect this rotation.
 - [18] T. Takeuchi *et al.*, J.Phys.Soc.Jap. **9**, 3255 (1992).
 - [19] B.Wolf *et al.*, unpublished.
 - [20] J. Sagi and I. Affleck, Phys.Rev.B **53**, 9188 (1996).
 - [21] M.P. Nightingale and H.W.J. Blöte, Phys.Rev.B **33**, 659 (1986).
 - [22] T. Sakai and M. Takahashi, Phys.Rev.B **42**, 4537 (1990).
 - [23] S.R. White, Phys.Rev.Lett. **69**, 2863 (1992); S.R. White, Phys.Rev.B **48**, 10345 (1993).
 - [24] Note that the angle θ contains a considerable error due to the experimental accuracy of the g-factor determination in eq. 2.